

DEVELOPMENT OF FILMS CONTAINING POLYLACTIC ACID/HALLOYSITE NANOTUBES IN BANANA ACTIVE PACKAGING

Aslı Beyler Çiğil¹ , Hatice Birtane² 

¹ Gazi University, Department of Chemistry and Chemical Process Technology,
Ankara, Turkey

² Marmara University, Department of Chemistry, Istanbul, Turkey

Abstract: Ethylene plays a significant role in the ripening and aging processes of fruits and vegetables, ultimately reducing their shelf life. Consequently, the presence of ethylene can restrict the marketability and consumer accessibility of certain horticultural products, leading to heightened post-harvest losses and increased food waste. In this study, nanocomposite packaging films with ethylene scavenging activity, which will help preserve freshness during distribution, were developed and tested as packaging for fresh products. Nanocomposite packaging films were prepared by adding different amounts of halloysite nanotubes (HNNTs) to polylactic acid (PLA). Structural characterization of nanocomposite packaging films was performed by FTIR. The thermal properties of nanocomposite packaging films in an inert atmosphere were studied using TGA. The nanocomposite films' surface energies, colours, transparency, and gloss were also measured. The nanocomposite films were printed with gravure and printability parameters were investigated. Finally, the effects of PLA/xHNNTs nanocomposite packaging films on the quality of packaged bananas were also monitored in terms of hardness, colour change, and weight loss. It has been observed that increasing the amount of HNNTs in PLA/xHNNT nanocomposite packaging films improves the storage time of bananas.

Key words: Active packaging, Protect fresh bananas, Polylactic acid, HNNT

1. INTRODUCTION

Food packaging is crucial in preserving food quality and safety, with plastics being widely used due to their affordability and effective sealing properties. However, petroleum-based plastics pose health risks through toxic residues and contribute to environmental pollution because of their nonbiodegradability. As a result, developing biodegradable alternatives has become a significant research focus, with many studies exploring the use of natural renewable resources such as polysaccharides, proteins, and lipids for innovative food packaging solutions (Zou et al., 2023; Wang et al., 2023; Yang et al., 2022). Polylactic acid (PLA) is a renewable and biodegradable biopolymer derived from resources like corn, making it a promising material for bio-composites and food packaging due to its good biocompatibility, low toxicity, and FDA approval (Boro et al., 2022; Villegas et al., 2017).

A key goal in food packaging is to reduce food loss by extending shelf life and ensuring the safe delivery of fresh, high-quality products. Active packaging, which interacts with the product, offers a promising alternative to traditional methods. These systems not only meet conventional packaging standards but also go beyond removing unwanted molecules, releasing beneficial components, or adjusting the packaging atmosphere. The specific needs of different food types have driven the development of diverse packaging systems to enhance preservation and safety (Alves et al., 2022; Durmaz et al., 2024).

Bananas are popular for their health benefits, containing dietary fibre, vitamins, minerals, phenolic compounds, and carotenoids (Xie et al., 2022; Qin et al., 2024). As a climacteric fruit, bananas undergo postharvest ripening, but harvesting them fully ripe complicates storage and transport due to their short shelf life. To address this, bananas are typically harvested before full ripeness and treated with exogenous stimuli to induce ripening, which shortens the market cycle and enhances their commercial value. While chemicals like calcium carbide and ethylene glycol have been used to ripen bananas, health concerns have led to a shift towards safer methods, such as controlled atmospheres and natural chemicals like ethylene and methyl jasmonate (Tao et al., 2021; Chai et al., 2022). However, ethylene poses safety hazards and can cause over-ripening, leading to significant economic losses (Xiao et al., 2024; Li et al., 2023). Ethylene scavenging is essential for maintaining the quality and shelf life of fruits and vegetables, as ethylene, even at low concentrations, accelerates ripening and deterioration. To address this, ethylene scavengers like potassium permanganate (KMnO₄) and metal catalysts, such as palladium, are commonly used in packaging. However, it is only applied in sachets rather than in direct contact with food due to the

toxicity of KMnO_4 (Alves et al., 2022; Janjarasskul & Suppakul, 2018). Other scavengers like activated carbon and zeolite raise safety concerns, particularly regarding accidental ingestion. Polymeric films incorporating ethylene scavengers have been developed as an alternative to sachets to improve safety and reduce costs (Sultana et al., 2023).

Nano clays, particularly halloysite nanotubes (HNNTs), show great promise as fillers in food packaging due to their hollow tubular structure, high aspect ratio, non-toxicity, abundance, and low cost. Widely used in applications like drug delivery and coatings, HNNTs enhance the thermal, mechanical, and barrier properties of polymer composites. Additionally, FDA-approved HNNTs can adsorb ethylene gas, helping to extend the shelf life of fruits and vegetables by improving the gas barrier and ethylene adsorption capabilities of packaging films (Kumar et al., 2023; Boonsiriwit et al., 2020).

In this study, food packaging films were developed by combining HNNTs with biobased and biodegradable PLA. This study aims to develop an environmentally friendly nanocomposite packaging film capable of extending the shelf life of bananas by capturing ethylene gas and regulating gas transfer. To achieve this, HNNTs were incorporated into the PLA matrix at varying concentrations (0-1-3 % wt.).

2. METHODS

2.1 Materials

Poly(lactic acid) (Mw $\sim 60,000$) used as a matrix was supplied from Sigma-Aldrich. The raw halloysite nanotubes were provided by ESAN, Eczacıbaşı, Türkiye. All solvents used in the experiments were of high purity and were obtained from Sigma Aldrich. Bananas were obtained from the local agricultural centre in Türkiye.

2.2 Preparation of PLA/HNNTs nanocomposite packaging films

PLA/HNNTs nanocomposite packaging films were produced by solvent casting, which does not need so much effort. HNNTs and PLA pellets were oven-dried under vacuum for 8 h at 80°C before starting the film preparation. For solvent casting, 10 g of PLA pellets were dissolved in 100 ml of chloroform for 4 h at room temperature with stirring at 1000 rpm on a magnetic stirrer. HNNTs were dispersed in a solution of PLA at a ratio of 0 (control film)–1–3 wt.% with a total solid content of 10 wt.% to prepare PLA/HNNTs nanocomposite packaging films. The film formulations to which HNNTs were added were kept in an ultrasonic bath for 30 minutes until the HNNTs became homogeneous. The formulations were cast onto glass Petri dishes (diam. 150 mm) and left to dry at room condition. The dried films were taken, a banana was packaged with each formulation, and the other films for testing were stored in a desiccator. Samples were coded according to HNNTs loading rates. For instance, PLA/1-HNNT represents the packaging film containing 1 wt.% HNNTs. The preparation scheme of PLA/HNNTs nanocomposite packaging films is given in Figure 1.

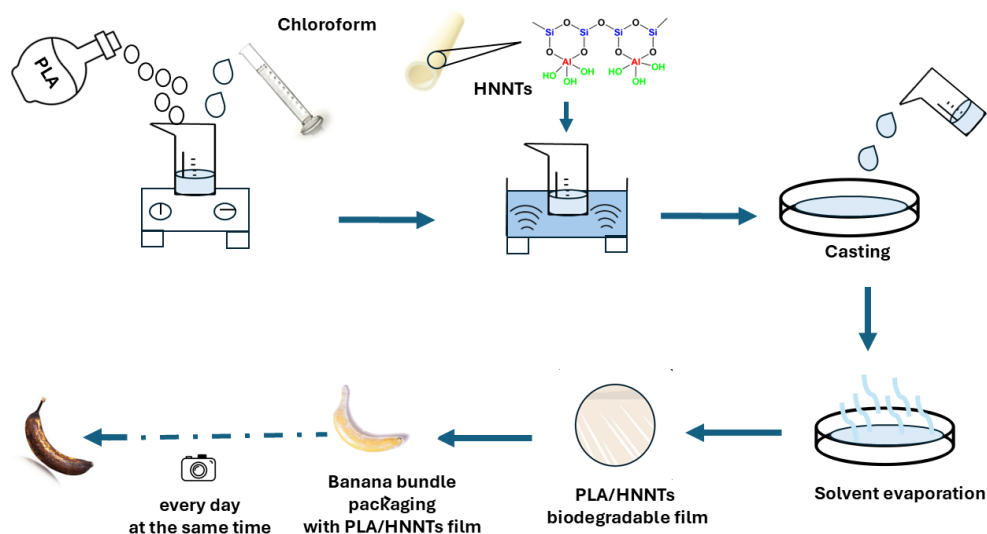


Figure 1: The preparation scheme of PLA/HNNTs nanocomposite packaging film

2.3 Characterization

Fourier-Transform Infrared Spectroscopy (FTIR) analysis was conducted using a Bruker IFS 66/S spectrometer equipped with ATR capability.

Thermal gravimetric analysis (TGA) was performed with a Perkin Elmer STA6000 instrument, with measurements carried out in the temperature range of 30°C to 750°C under a nitrogen atmosphere at a heating rate of 10°C/min.

The colours of the obtained nanocomposite packaging films were measured by X-Rite eXact portable spectrophotometer according to the ISO 13655:2017 standard. The measurement conditions of the spectrophotometer were determined as a polarization filter with 0/45° geometry with a 2° observer angle and a D50 light source in the range of 400-700 nm.

Colour differences were calculated using the CIE Lab (2000) technique (Equation 1). ISO 11664-6:2014. Calculations were performed by calculating the average of five measurements. ΔL^* , Δa^* , and Δb^* : Difference in L^* , a^* , and b^* values between the specimen and target colours, respectively. The lightness is represented by the L^* axis, which ranges from white to black. The red area is connected to green by the a^* axis, whereas the b^* axis runs from yellow to blue.

$$\Delta E_{00}^* = \sqrt{\left(\frac{\Delta L'}{k_L S_L}\right)^2 + \left(\frac{\Delta C'}{k_C S_C}\right)^2 + \left(\frac{\Delta H'}{k_H S_H}\right)^2 + R_T \frac{\Delta C'}{k_C S_C} \frac{\Delta H'}{k_H S_H}} \quad (1)$$

Where ΔL^* , ΔC^* , and ΔH^* are the CIE $L^*a^*b^*$ metric lightness, chroma, and hue differences, respectively, calculated between the standard and sample in a pair, and ΔR is the interaction term between the chroma and hue differences. S_L , S_C , and S_H are the weighting functions for lightness, chroma, and hue components. The values calculated for these functions vary according to the positions of the sample pair considered in the CIE $L^*a^*b^*$ colour space. The k_L , k_C , and k_H values are the parametric factors to be adjusted according to different viewing parameters, such as textures, backgrounds, and separations, for the lightness, chroma, and hue components.

The gloss measurements of all nanocomposite packaging films were carried out with the BYK Gardner GmbH micro gloss 75° geometry by ISO 8254-1:2009. The contact angles of nanocomposite packaging films were found on Pocket Goniometer Model PG-X, version 3.4 (FIBRO Systems AB, Sweden).

Surface-free energy was calculated according to the ASTM D5946 standard test method, depending on the water contact angle. The images of droplets were then recorded by using a CCD video camera.

The transparency of the nanocomposite packaging films was examined visually. Gravure prints were made on the obtained films with SEIGWERK ethyl alcohol solvent blue 20 seconds viscosity ink at 1m/s printing speed with RK printing proofer, and the colour properties of the obtained prints were determined by X-Rite eXact portable spectrophotometer according to the ISO 13655:2017 standard.

To examine the storage of fresh bananas using nanocomposite packaging films, bananas were obtained from the local agricultural centre in Türkiye. Fresh bananas were characterized by a green-yellow colour (80 % ripening stage), where unblemished, rot-free, well-formed bananas were selected. Three selected bananas of the same maturity were placed in the middle of the dried nanocomposite packaging film with three different contents. The bananas were tightly wrapped with nanocomposite packaging films. All specimens were stored at room temperature and the same relative humidity and were examined both visually and tactilely daily.

3. RESULTS AND DISCUSSIONS

3.1 Structural characterization of the nanocomposite packaging films

FTIR spectroscopy can be used to characterize the identification of specific functional groups in the nanocomposite packaging films. Figure 2 shows the FTIR spectra of pure PLA, HNNTs, and PLA nanocomposite packaging films with 1, and 3, wt.% HNNTs. For pure PLA films and nanocomposite PLA films with 1, and 3, wt.% HNNTs, the representative bands were detected at 2800-3000 cm^{-1} from CH_2 asymmetric stretching, at 3400–3000 cm^{-1} for the O–H stretch, and 1750 and 1180 cm^{-1} , which belong to the C=O stretching and the C–O–C stretching. Looking at Figure 2, the FTIR spectrum of HNNTs can be seen. HNNTs have specific absorption bands at 3600 and 911 cm^{-1} due to O-H stretching and Al-O-OH bending. Moreover, the specific planar stretching vibration at 1091 cm^{-1} and 1034 cm^{-1} seen in HNNTs is due to the presence of Si–O–Si. The peak characteristic of Si–O–Si bonds became more pronounced with

the increasing HNNT content in the nanocomposite packaging films, which can be attributed to the silicon and oxygen composition of the HNNTs.

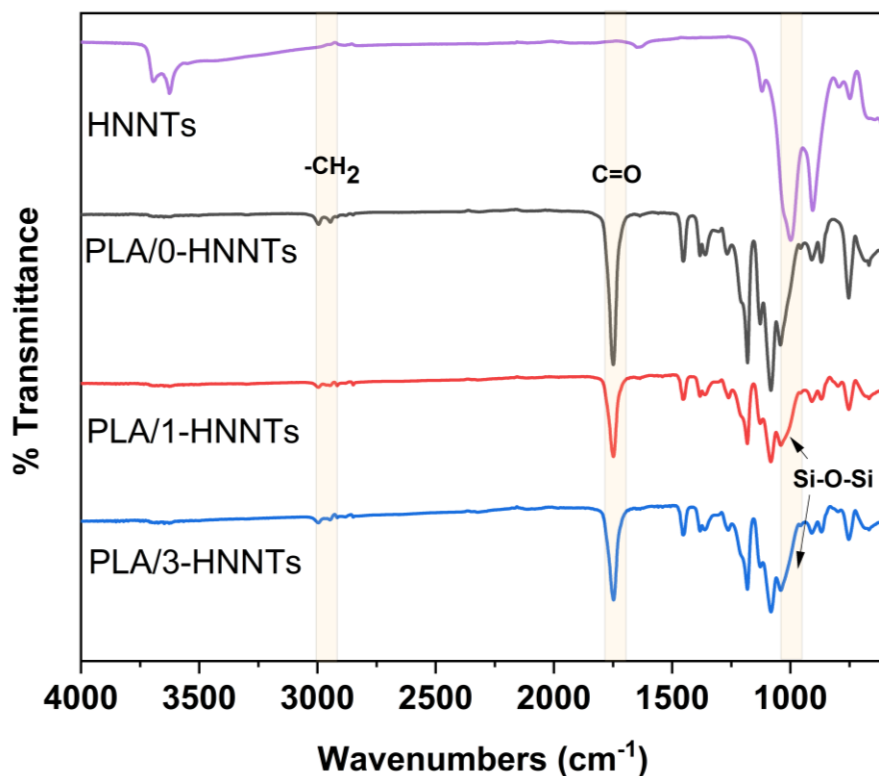


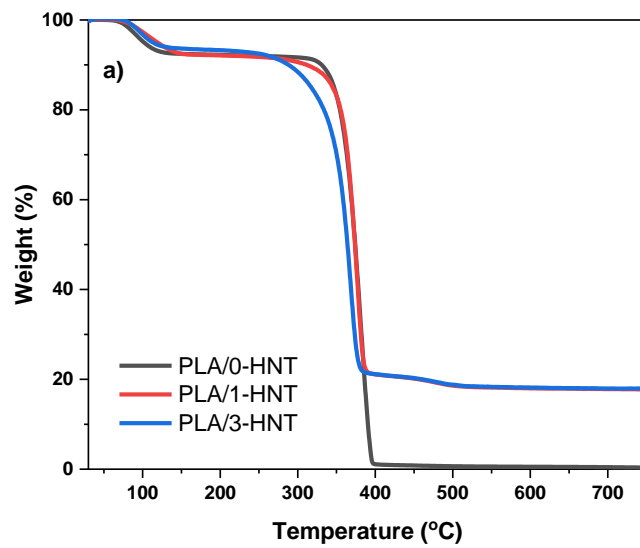
Figure 2: FTIR spectra of PLA/HNNTs nanocomposite loaded with 0, 1, and 3, wt% HNNTs. The spectrum for HNNTs is shown for comparison

3.2 Thermal characterization of the nanocomposite packaging films

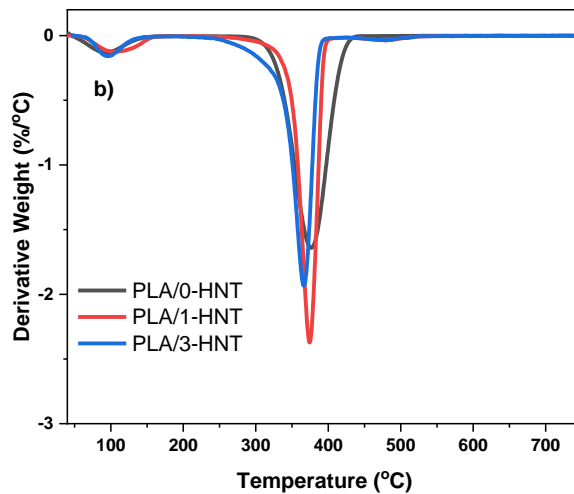
Figure 3 shows the TGA curves of the nanocomposite packaging films (PLA/x-HNNTs). The TGA results are summarized in Table 1. The maximum degradation temperature of PLA films without HNNTs is 377 °C. The thermal decomposition of PLA is mainly due to chain depolymerization (Lim et al., 2019). The results indicate that increasing the loading amount of HNNTs into PLA gradually decreased the degradation temperature, which was reduced from 377 °C (PLA/0-HNNTs) to 364 °C for the film containing 3% HNNTs. The incorporation of HNNTs into the nanocomposite packaging films did not enhance their thermal stability. This is attributed to the lower insulation efficiency of HNNTs in comparison to other silicate nanolayers, primarily due to their tubular structure. Consequently, at low loading ratios, they fail to effectively stabilize the polymer matrix (Du et al., 2006). As expected, the % char content at 750 °C of nanocomposite packaging films increased with the loading amount of HNNTs. The char yield of the nanocomposite films containing 0%, 1%, and 3% HNNTs was determined to be 0.3%, 17.74%, and 17.83%, respectively.

Table 1: TGA results of PLA/0-HNNTs, PLA/1-HNNTs, and PLA/3-HNNTs nanocomposite packaging films

	T ₅ (°C)	T _{max1} (°C)	T _{max2} (°C)	Char
PLA/0-HNNTs	98	94	377	0.3
PLA/1-HNNTs	114	106	374	17.74
PLA/3-HNNTs	108	97	364	17.83



a)



b)

Figure 3: a) TGA curves of PLA/0-HNNTs, PLA/1-HNNTs, and PLA/3-HNNTs nanocomposite packaging films, b) DTG curves of PLA/0-HNNTs, PLA/1-HNNTs, and PLA/3-HNNTs nanocomposite packaging films

3.2 Colour properties of the nanocomposite packaging film

A simple naked-eye investigation of these images reveals that the transparency and colour characteristics of the pure PLA films were highly transparent and glossy. However, HNNTs were added to the formulation, and nanocomposite packaging films became semi-transparent and slightly yellow. Despite this change, the texts can still be read. Table 2 shows the colour $L^*a^*b^*$ coordinate values, the colour difference (ΔE_{ab^*}), and glosses of the PLA/0-HNNTs, PLA/1-HNNTs, and PLA/3-HNNTs nanocomposite packaging films.

Table 2: Colour properties of PLA/0-HNNTs, PLA/1-HNNTs, and PLA/3-HNNTs nanocomposite packaging films

	L	a	b	Delta E	Glos
PLA/0-HNNTs	90,29	1,89	-6,85	Reference	86,6
PLA/1-HNNTs	88,40	1,84	- 4,12	2,54	57,1
PLA/3-HNNTs	85,10	1,57	-1,521	5,63	45,5

When the colour values in Table 2 are analyzed, it is seen that there is not much change in the (green and red) value of the nanocomposite packaging films with HNNTs added compared to the pure PLA film (PLA/0-HNNTs), and the biggest difference is in the b (blue and yellow) value. This difference shows itself as a shift towards yellow. The reason for this shift towards yellow is due to the titaniferous content in the HNNTs. When the colour differences are analyzed, it is determined that PLA/1-HNNTs "does not have a noticeable colour difference" (Delta E is less than 3), but the colour difference of PLA/3-HNNTs increases with the addition of more HNNTs, and "the two colours are not the same colour" (Delta E is less than 5). As a result, the colour changes towards yellow as the amount of HNNTs increases. When the gloss values are analyzed, it is determined that the pure film has a very high gloss, the surface roughness increases with the addition of HNNTs, and accordingly the light is scattered and the gloss decreases. The results are supported by the literature. (Rojas-Lema et al., 2020; Trezza et al., 2001).

3.3 Surface properties of the nanocomposite packaging film

The contact angles and surface energies of the produced nanocomposite packaging films were investigated and shown in Figure 4. When Figure 4 was examined, the contact angle of the PLA/0-HNNTs nanocomposite packaging film was measured as 74.9°. This is a very close result to the contact angle values in the literature (Silva et al., 2014). A decrease in the contact angle (PLA/1-HNNTs: 72°, PLA/3-HNNTs: 64.9°) can be seen with the addition of HNNTs into the PLA packaging film. This is thought to occur because of the increase in surface energy by the hydroxyl groups of HNNTs increasing the polarity of the film. This decrease becomes a little more pronounced as the amount of HNNTs increases in the two concentrations in this study. In the literature, it is stated that when higher HNNT ratios are studied, the decrease in surface energy due to surface roughness dominates the polarity, therefore the contact angle starts to increase after 7 wt.% HNNTs ratios. The relevant results are consistent with the literature (Alakrach et al., 2018).

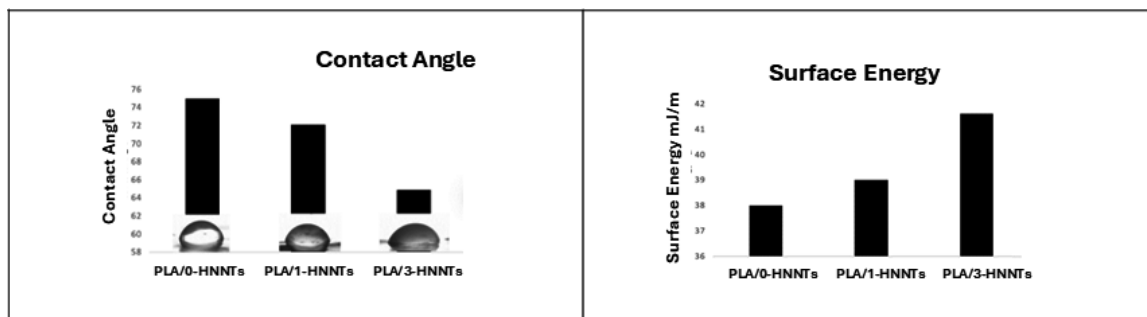


Figure 4: Contact angles and surface energies of PLA/0-HNNTs, PLA/1-HNNTs, and PLA/3-HNNTs nanocomposite packaging films

As illustrated in Figure 5, translucent, flexible nanocomposite packaging films were produced by solvent casting method. PLA/0-HNNTs (only PLA) nanocomposite packaging films are fully transparent. HNNTs ingredient PLA films are semitransparent and contains of whitish macroscopic spots. This situation is tough due to the nucleating effect of HNNTs and could resemble the 'micro-nano binary' structure the same line as that Liu et al noticed for polypropylene/HNT composites (Liu et al., 2010).



Figure 5: Images of PLA/0-HNNTs, PLA/1-HNNTs, and PLA/3-HNNTs nanocomposite packaging films

3.4 Printability properties of the nanocomposite packaging film

Prints were successfully made with blue ink on the three different nanocomposite packaging films obtained. No viscosity problems were experienced during the prints. The results of the adhesion test with the tape after the prints dried revealed that the adhesion was high for commercial ink, as there was no ink residue on the tape. The colour properties of the prints obtained are given in Table 3. When Table 3 is examined, it can be concluded that the addition of HNNTs shifted the colour of the nanocomposite packaging films to yellow, and the prints shifted slightly to yellow with the shift in the b-axis. This yellow shift in colour is due to the titaniferous compounds found in the chemical content of HNNTs. However, the colour change (delta e) is below 3, which means it is quite difficult to perceive by eye. As the amount of HNNTs in the nanocomposite packaging films increased, the yellow shift in the print and the amount of delta e increased, but there is no correlation between the increment. The results are compatible with the literature (Rojas-Lema et al., 2020).

Table 3: Colour properties of printed nanocomposite packaging films

	L	a	b	Delta E	Image
PLA/0-HNNTs	47	-10	-42	Reference	
PLA/1-HNNTs	45	-8	-40	1,90	
PLA/3-HNNTs	44	-8	-38	2,19	

3.5 Storage studies of the nanocomposite packaging film

As a climacteric fruit, bananas continue to undergo the ripening process after harvesting due to the release of ethylene gas. Considering this phenomenon, the impact of ethylene release on the browning and decay of fresh bananas was evaluated through photographic documentation after a 12-day storage period. Figure 6 presents photographs of bananas packaged in nanocomposite films over a 12-day period. Among the packaging films tested, PLA/3-HNNTs nanocomposite films exhibited the highest ethylene scavenging ability, followed closely by PLA/1-HNNTs nanocomposite films. As illustrated in Figure 6, bananas packaged in pure PLA began to darken after 8 days. In contrast, the bananas packaged in PLA/3-HNNTs and PLA/1-HNNTs films retained a closer resemblance to their initial appearance. While the bananas wrapped in PLA/1-HNNTs films began to show signs of darkening, those packaged in PLA/3-HNNTs films maintained their initial appearance and remained undecayed for the entire 12-day period at room temperature.

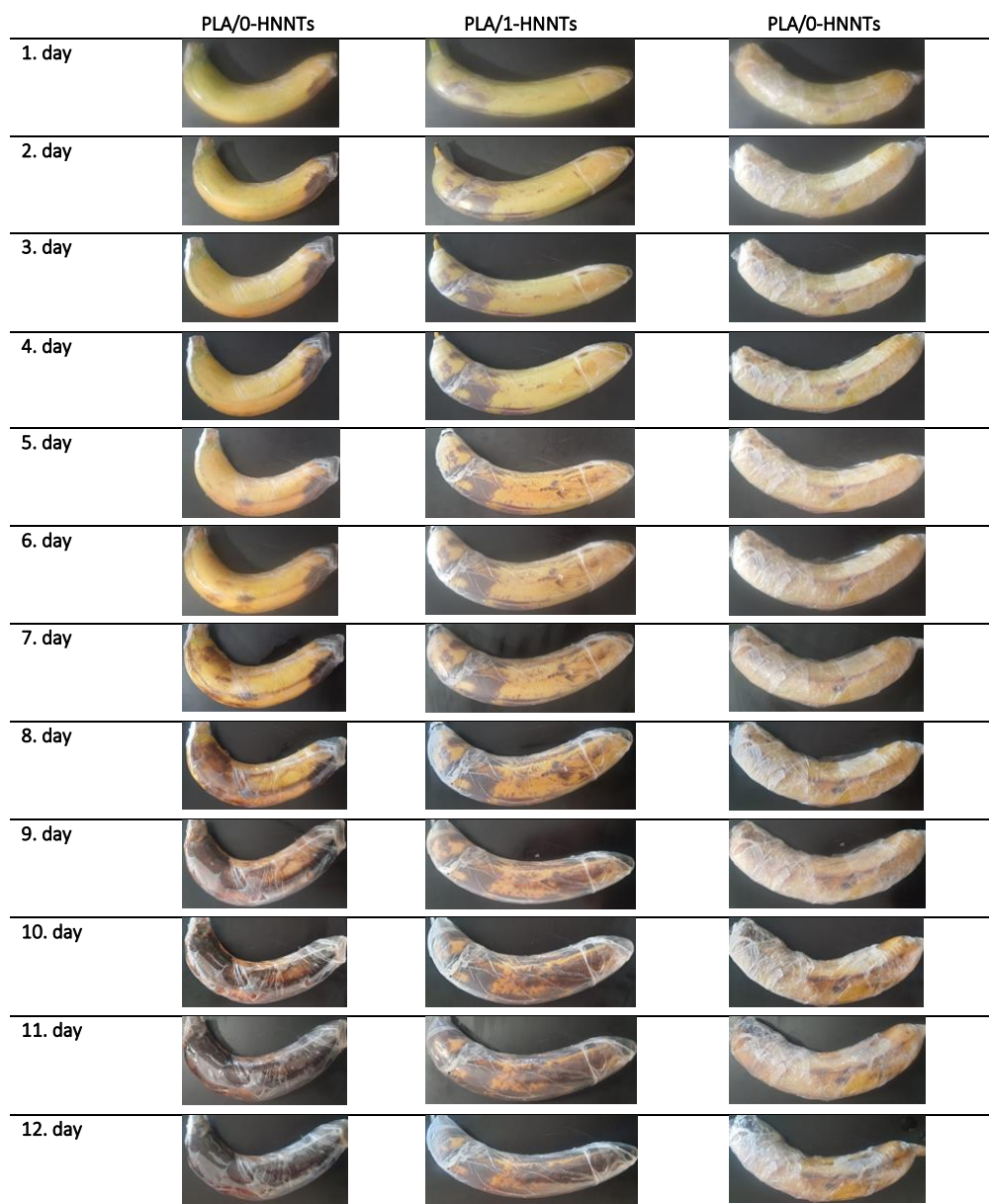


Figure 6: Effects of PLA/HNNTs nanocomposite packaging films

5. CONCLUSIONS

In this study, HNNTs-reinforced PLA nanocomposite packaging films were developed as potential eco-friendly, ethylene-scavenging active packaging materials for bananas. The nanocomposite packaging films were prepared by solvent casting, which is an easy production method. The impacts of HNNTs content were investigated on the structural, thermal, printability properties, surface properties, and ethylene scavenging ability of the nanocomposite packaging films. The incorporation of HNNTs was found to enhance the ethylene scavenging ability of PLA. It was concluded that the produced nanocomposite packaging films were transparent and semi-transparent and that the addition of HNNTs shifted the film colour slightly to yellow. It was determined that all of the obtained *nanocomposite packaging* films were printed with commercial ink without any problems and had good printability characteristics. Finally, the effects of the films on bananas were examined, and it was determined that films containing 3 wt.% HNNTs are suitable as packaging materials for bananas. Considering their physical and functional properties, PLA/3-HNNTs nanocomposite packaging films exhibit considerable potential as a viable alternative to synthetic packaging materials and as effective ethylene scavengers for fresh fruit packaging.

7. REFERENCES

- Alakrach, A. M., Noriman, N. Z., Dahham, O. S., Hamzah, R., Alsaadi, M. A., Shayfull, Z. & Syed Idrus, S. Z. (2018) Chemical and Hydrophobic Properties of PLA/HNTs-ZrO₂ Bionanocomposites. *In Journal of Physics: Conference Series*. 1019 (2018), 012065
- Alves, J., Gaspar, P. D., Lima, T. M., Silva, P. D. (2022) What is the role of active packaging in the future of food sustainability? A systematic review. *Journal of the Science of Food and Agriculture*. 103, 1004 - 1020. Available from: <https://doi.org/10.1002/jsfa.11880>
- Boonsiriwit, A., Xiao, Y., Joung, J., Kim, M., Singh, S. & Lee, Y. S. (2020) Alkaline halloysite nanotubes/low density polyethylene nanocomposite films with increased ethylene absorption capacity: applications in cherry tomato packaging. *Food Packaging and Shelf Life*. 25, 100533. Available from: <https://doi.org/10.1016/j.fpsl.2020.100533>
- Boro, U., Priyadarsini, A. & Moholkar, V. (2022) Synthesis and characterization of poly(lactic acid)/clove essential oil/alkali-treated halloysite nanotubes composite films for food packaging applications. *International Journal of Biological Macromolecules*. 216, 927 - 939. Available from: <https://doi.org/10.1016/j.ijbiomac.2022.07.209>
- Chai, J., Wang, Y., Liu, Y., Gu, Z. & Liu, Z. (2022) High O₂/N₂ controlled atmosphere accelerates postharvest ripening of 'Hayward' kiwifruit. *Scientia Horticulturae*. 300, 111073, Available from: <https://doi.org/10.1016/j.scienta.2022.111073>
- De Silva, R. T., Pasbakhsh, P., Goh, K. L., Chai, S. P. & Chen, J. (2014) Synthesis and characterisation of poly(lactic acid)/halloysite bionanocomposite films. *Journal of Composite Materials*. 48, 3705 - 3717. Available from: <https://doi.org/10.1177/0021998313513046>
- Du, M., Gao, D. & Jia, D. (2006) Thermal stability and flame retardant effect of halloysite nanotubes on poly(propylene). *European Polymer Journal*. 42, 1362. Available from: <https://doi.org/10.1016/j.eurpolymj.2005.12.006>
- Janjarasskul, T. & Suppakul, P. (2018) Active and intelligent packaging: the indication of quality and safety. *Critical Reviews in Food Science and Nutrition*. 58, 808 - 831. Available from: <https://doi.org/10.1080/10408398.2016.1225278>
- Kumar, A., Ramakanth, D., Akhila, K. & Gaikwad, K. K. (2023) Influence of halloysite nanotubes/microfibrillated cellulose on pine leaves waste based ethylene scavenging composite paper for food packaging applications. *Applied Clay Science*. 231, 106726. Available from: <https://doi.org/10.1016/j.clay.2022.106726>
- Li, X., Xiong, T., Zhu, Q., Zhou, Y., Lei, Q., Lu, H. & Zhu, X. (2023) Combination of 1-MCP and modified atmosphere packaging (MAP) maintains banana fruit quality under high temperature storage by improving antioxidant system and cell wall structure. *Postharvest Biology and Technology*. 198, 112265. Available from: <https://doi.org/10.1016/j.postharvbio.2023.112265>
- Lim, K., Chow W. S. & Pung, S. Y. (2019) Accelerated Weathering and UV Protection-Ability of Poly(lactic acid) Nanocomposites Containing Zinc Oxide Treated Halloysite Nanotube. *Journal of Polymers and the Environment*. 27, 1746 – 1759. Available from: <https://doi.org/10.1007/s10924-019-01464-5>
- Liu, M., Jia, Z., Liu, F., Jia, D. & Guo, B. (2010) Tailoring the wettability of polypropylene surfaces with halloysite nanotubes. *Journal of Colloid and Interface Science*. 350, 186 - 193. Available from: <https://doi.org/10.1016/j.jcis.2010.06.047>
- Qin, Z., Jiang, Q., Chen, M., Li, J. & Zhang, H. (2024) Food packaging for ripening and preserving banana based on ethylene-loaded nanofiber films deposited with nanosized cyclodextrin metal-organic frameworks and TiO₂ nanoparticles. *Food Packaging and Shelf Life*. 45, 101332. Available from: <https://doi.org/10.1016/j.fpsl.2024.101332>
- Rojas-Lema, S., Quiles-Carrillo, L., Garcia-Garcia, D., Melendez-Rodriguez, B., Balart, R. & Torres-Giner, S. (2020) Tailoring the properties of thermo-compressed polylactide films for food packaging applications by individual and combined additions of lactic acid oligomer and halloysite nanotubes. *Molecules*. 25, 1976. Available from: <https://doi.org/10.3390/molecules25081976>

- Sultana, A., Kumar, L. & Gaikwad, K. K. (2023) Lignocellulose nanofibrils/guar gum-based ethylene scavenging composite film integrated with zeolitic imidazolate framework-8 for food packaging. *International Journal of Biological Macromolecules*. 243, 125031. Available from: <https://doi.org/10.1016/j.ijbiomac.2023.125031>
- Tao, X., Wu, Q., Li, J., Wang, D., Nassarawa, S. S. & Ying, T. (2021) Ethylene biosynthesis and signal transduction are enhanced during accelerated ripening of postharvest tomato treated with exogenous methyl jasmonate. *Scientia Horticulturae*. 281, 109965. Available from: <https://doi.org/10.1016/j.scienta.2021.109965>
- Trezza, T. A. & Krochta, J. M. (2001) Specular reflection, gloss, roughness and surface heterogeneity of biopolymer coatings. *Journal of Applied Polymer Science*. 79, 2221 - 2229. Available from: [https://doi.org/10.1002/1097-4628\(20010321\)79:12<2221::AID-APP1029>3.0.CO;2-F](https://doi.org/10.1002/1097-4628(20010321)79:12<2221::AID-APP1029>3.0.CO;2-F)
- Ucpinar Durmaz, B., Ugur Nigiz, F. & Aytac, A. (2024) Active packaging films based on poly(butylene succinate) films reinforced with alkaline halloysite nanotubes: Production, properties, and fruit packaging applications. *Applied Clay Science*. 259, 107517. Available from: <https://doi.org/10.1016/j.clay.2024.107517>
- Villegas, C., Torres, A., Rios, M., Rojas, A., Romero, J., Dicastillo, de C. L. & Guarda, A. (2017) Supercritical impregnation of cinnamaldehyde into polylactic acid as a route to develop antibacterial food packaging materials. *International Food Research Journal*. 99, 650 - 659. Available from: <https://doi.org/10.1016/j.foodres.2017.06.031>
- Wang, F., Xie, C., Ye, R., Tang, H., Jiang, L. & Liu, Y. (2023) Development of active packaging with chitosan, guar gum and watermelon rind extract: characterization, application and performance improvement mechanism. *International Journal of Biological Macromolecules*. 227, 711 - 725. Available from: <https://doi.org/10.1016/j.ijbiomac.2022.12.210>
- Xiao, F., Xiao, Y., Ji, W., Li, L., Zhang, Y., Chen, M. & Wang, H. (2024) Photocatalytic chitosan-based bactericidal films incorporated with WO₃/AgBr/Ag and activated carbon for ethylene removal and application to banana preservation. *Carbohydrate Polymers*. 328, 121681. Available from: <https://doi.org/10.1016/j.carbpol.2023.121681>
- Xie, J., Wang, R., Li, Y., Ni, Z., Situ, W., Ye, S. & Song, X. (2022) A novel Ag₂O-TiO₂-Bi₂WO₆/polyvinyl alcohol composite film with ethylene photocatalytic degradation performance towards banana preservation. *Food Chemistry*. 375, 131708. Available from: <https://doi.org/10.1016/j.foodchem.2021.131708>
- Yang, Z., Zhai, X., Zhang, C., Shi, J., Huang, X., Li, Z., Zou, X., Gong, Y., Holmes, M., Povey, M. & Xiao, J. (2022) Agar/TiO₂/radish anthocyanin/neem essential oil bionanocomposite bilayer films with improved bioactive capability and electrochemical writing property for banana preservation. *Food Hydrocolloids*. 123, 107187. Available from: <https://doi.org/10.1016/j.foodhyd.2021.107187>
- Zou, Y., Sun, Y., Shi, W., Wan, B. & Zhang, H. (2023) Dual-functional shikonin-loaded quaternized chitosan/polycaprolactone nanofibrous film with pH-sensing for active and intelligent food packaging. *Food Chemistry*. 399, 133962. Available from: <https://doi.org/10.1016/j.foodchem.2022.133962>



© 2024 Authors. Published by the University of Novi Sad, Faculty of Technical Sciences, Department of Graphic Engineering and Design. This article is an open access article distributed under the terms and conditions of the Creative Commons Attribution license 3.0 Serbia (<http://creativecommons.org/licenses/by/3.0/rs/>).